AHU Doctor: An inverse model-based software platform for commissioning controls hardware and sequences in VAV AHU systems

Burak Gunay[1], Darwish Darwazeh[1,2], Narges Torabi[1], Scott Shillinglaw[2]
[1]Civil and Environmental Engineering, Carleton University, Ottawa, Canada
[2]Construction Research Centre, National Research Council, Ottawa, Canada

Abstract

Faults in variable air volume (VAV) air handling unit (AHU) system control hardware and software detrimentally affect indoor environmental quality and energy performance. Existing fault detection and diagnostics (FDD) platforms employ simplistic expert rules, offer limited visualization capabilities to their end-users, and do not utilize state-of-the-art FDD approaches. This paper presents an inverse model-based FDD tool for commissioning controls hardware and sequences in VAV AHU systems. The software tool inputs widely available building automation system trend data types to train inverse models characterizing the heat and air mass balance of a VAV AHU system. The models are then used to detect nine common controls hardware and sequence logic faults. The platform is demonstrated with data from a 69-zone VAV AHU system in Ottawa, Canada. Five of the nine fault categories are detected and confirmed to be present in the case study building.

Introduction

Delivery of heating, ventilation, and air-conditioning (HVAC) services inside large buildings requires control systems with thousands of sensors, actuators, and programs responsible for automating many interconnected systems and equipment. Thus, energy efficiency and indoor environmental quality (IEQ) of a large building strictly depend on the health of HVAC control systems, which can deteriorate over time as faults emerge.

HVAC control system faults can be broadly categorized into two groups: hard and soft faults. Hard faults occur as controls hardware (sensors and actuators) naturally age causing functional errors in their systems and readings. Soft faults are due to human errors in the initial programming of a building automation system (BAS) or changes to programming during regular building operations.

Large-scale commissioning studies revealed that HVAC control system faults waste 15 to 20% of total energy use in commercial and institutional buildings (Claridge et al., 2004; Mills, 2011; Mills et al., 2005). These savings were achieved through simple corrections to the sequences of operation such as implementing supply air temperature (SAT) and duct static supply air pressure (SAP) reset, adjusting start/stop scheduling and temperature setpoints, and by addressing hardware faults such as fixing leaky outdoor air dampers, failed valve actuators, and recalibrating temperature sensors. Hard and soft faults were found to cause simultaneous heating and cooling, improper economizer sequence, erroneous fan speeds and scheduling, and equipment staging and control loop tuning issues.

HVAC control system faults have been traditionally identified through retro-commissioning, whereby in-house energy managers or external consultants manually analyze amorphous datasets extracted from the BAS. FDD methods formalize the commissioning process of HVAC control systems. There has been significant research to develop FDD methods since 1990s. The early examples were largely expert rulesets (Schein et al., 2006). These expert rulesets have been criticized for generating too many false positives (Bruton et al., 2015). Because it is difficult to formulate expert rulesets comprehensively overarching zone-to-system-level interactions without inverse modelling, a fault may trigger many false alarms while masking true faults (Mirnaghi & Haghighat, 2020). Thus, the majority of the recent examples from the literature employ inverse greybox and blackbox model-based FDD methods (Kim & Katipamula, 2018). Inverse model-based FDD methods are considered more generalizable and accurate than expert rulesets, if the models are structured appropriately (Shi & O'Brien, 2019).

Despite the strides made in inverse model-based FDD methods, expert rulesets are still the industry standard for FDD applications. They are within ASHRAE Guideline 36 (2018) and are used in numerous commercial FDD software (Granderson et al., 2018). To this end, this paper introduces a prototype software tool *ahuDoctor*, which is built upon existing inverse model-based FDD algorithms from the literature (Darwazeh et al., 2021; Gunay et al., 2022a; Gunay et al., 2022b; Gunay et al., 2020; Torabi et al., 2021). The software tool is compiled as a standalone application. It inputs common BAS trend data types from a multiple-zone VAV AHU system. It outputs hard and soft fault alarms, visualizations displaying ideal and measured operation patterns, and a key performance indicator (KPI). The scope is limited to multiple-zone VAV AHU systems, considering their widespread use in commercial and institutional buildings across North America and the fact that they are custom designed, assembled, and programmed, thus prone to having faults.

FDD tool architecture

Fig. 1 presents the BAS data points required by the software tool on a generic multiple zone VAV AHU system. At the AHU level, it inputs trend data for outdoor (T_{oa}), return (T_{ra}) and supply air temperatures (T_{sa}), supply air pressure (P_{sa}), mixing box damper command ($s_{mb,dp}$), heating (s_{hc}) and cooling (s_{cc}) coil valve states, and supply fan state (s_{fan}). In addition, from each VAV zone served by the AHU, it inputs the following trend data: VAV terminal unit damper position (s_{dp}), discharge airflow rate (q_{vav}) and airflow setpoint (q_{vav-sp}), and zone temperature (T_{in}). The input data must be between six months and a year in length at hourly intervals.

The FDD tool also requires two user inputs: minimum mixing box damper position setpoint $s_{mb,dp-sp}$ and seasonal availability of the heating and cooling. The tool first detects system-level hardware faults affecting the mixing box damper and heating and cooling coil valves. It subsequently detects zone-level faults affecting VAV terminal units and zone airflow and temperature control. Finally, it detects sequencing logic faults affecting the state and mode of operation of the system as well as SAT and SAP setpoint reset behaviours. The remainder of this section explains the back-end FDD algorithms of the software tool and their implementation as a standalone application.

Detection of system-level hardware faults

<u>Mixing box dampers</u>

In order to detect a hardware fault affecting the mixing box dampers, the relationship between the outdoor air fraction in the supply air (f_{oa}) and $s_{mb,dp}$ is modelled as follows (Gunay et al., 2022):

$$f_{oa} = \frac{x_{3,mb}}{exp(x_{1,mb} \cdot s_{mb,dp} + x_{2,mb})} \quad (1)$$

where $\boldsymbol{x}$ is the unknown parameters of the model, and the subscript mb stands for the mixing box.

Because f_{oa} is an unmeasured quantity in most AHUs and humidity sensors monitoring return, outdoor, and mixed air are not always available, it is approximated as follows (Najafi et al., 2012; Shea et al., 2019):

$$f_{oa} = \frac{T_{ma} - T_{ra}}{T_{oa} - T_{ra}} \quad (2)$$

where T_{ma} (°C) is the mixed air temperature. Because mixed air temperature is not always present, after excluding timesteps when heating and cooling coils are on, T_{ma} is approximated as follows:

$$T_{ma} = T_{sa} - \left(\frac{P_{sa}}{\rho \cdot c_p \cdot \eta}\right) \quad (3)$$

Note that the term $\frac{P_{sa}}{\rho \cdot c_p \cdot \eta}$ represents the temperature rise across the supply fan, where ρ (kg/m^3) and c_p (J/kg°C) are density and specific heat of air, respectively, and η is the fan efficiency (Padilla et al., 2015).

The parameters of Eqn. 1 are solved using the genetic algorithm with a population size of 5000 in ten generations. A mixing box damper fault is detected if the parameter estimates of Eqn. 1 result in a f_{oa} and $s_{mb,dp}$ relationship outside acceptable range as per AMCA (2009).

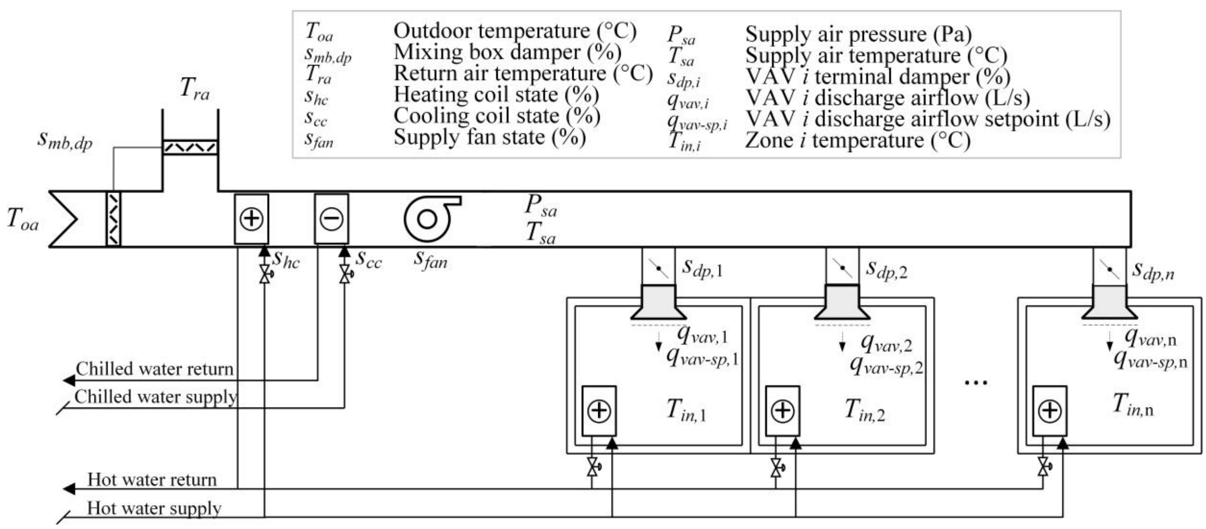

Figure 1: BAS points required by the software tool on a generic multiple zone VAV AHU system.

<u>Heating and cooling coil valve</u>

In order to detect a heating or a cooling coil valve fault, the temperature rise and drop across the heating and cooling coils are represented as a function of the heating and cooling coil valve position (Gunay et al., 2022):

$$T_{sa} - T_{ma} = \frac{x_{3,hc/cc}}{exp\left(x_{1,hc/cc} \cdot s_{hc/cc} + x_{2,hc/cc}\right)} \quad (4)$$

Note that T_{ma} can be estimated by using the trained mixing box model (Eqn. 1) and Eqn. 2.

The parameters of Eqn. 4 are solved using the genetic algorithm with a population size of 5000 in ten generations. A heating coil valve fault is detected if trained Eqn. 4 predicts a temperature rise less than 5°C across a fully open heating coil valve. Similarly, if the predicted temperature drop is less than 5°C across a fully open cooling coil valve, a cooling coil valve fault alarm is generated.

Detection of zone-level faults

VAV terminal unit damper

In order to detect a VAV terminal unit damper fault, the relationship between the airflow rate at a VAV terminal and VAV terminal's damper position and AHU SAP is modelled as follows (Gunay et al., 2022):

$$q_{vav,i} = \left(s_{dp,i} \cdot x_{1,vav,i} + x_{2,vav,i}\right) \cdot \sqrt{P_{sa}} \quad (5)$$

where subscript i stands for the index number of the zone. Note the proportionality between $\sqrt{P_{sa}}$ and $q_{vav,i}$ is as per Bernoulli's principle. The unknown parameters of Eqn. 5 are estimated by using the method of iteratively reweighted least squares. If the parameter estimate $x_{1,vav,i}$ is negative, a VAV terminal unit fault alarm is generated for zone i.

Zone airflow and temperature control

As described by Markus et al. (2021), a zone airflow fault alarm is generated if the normalized airflow control error $\left(\frac{mean(|q_{vav,i} - q_{vav-sp,i}|)}{max(q_{vav-sp,i})}\right)$ for zone i exceeds 20%. A temperature control fault alarm is generated if mean summer or winter temperature for zone i is more than 25°C or less than 20°C, respectively.

Detection of sequences of operation faults

State of operation

The state of operation of a VAV AHU system is divided into four states by a split-range controller, namely, heating, economizer, economizer with cooling, and cooling states (ASHRAE, 2018). If the SAT setpoint is between the return and outdoor air temperatures, an AHU is expected to operate in the economizer state. At this state, the SAT setpoint can be met by simply modulating the mixing box dampers without using the heating and cooling coils. If the outdoor air temperature is less than the return air temperature but more than the SAT setpoint, an AHU is expected to operate in the economizer with cooling state. In this state, as the outdoor air is closer to the intended SAT than the return air, the mixing box damper opens fully to operate at 100% outdoor air. However, cooling coil operation is necessary to bring the outdoor temperature to the SAT setpoint. If these two conditions are not met, the AHU is expected to operate in the heating or cooling states. In these states, the mixing box damper command signal is kept at its minimum position setpoint $s_{mb,dp,minsp}$. The following equation summarizes the expected mixing box damper position behaviour $s_{mb,dp,exp}$:

$$s_{mb,dp,exp} = \begin{cases} 1, & T_{sa} \leq T_{oa} \leq T_{ra} \\ \dfrac{\ln\left(\dfrac{x_{3,mb}}{\frac{T_{ma} - T_{ra}}{T_{oa} - T_{ra}}}\right) - x_{2,mb}}{x_{1,mb}}, & T_{oa} \leq T_{sa} \leq T_{ra} \\ s_{mb,dp,minsp}, & \text{otherwise.} \end{cases} \quad (6)$$

Recall that the term $\frac{T_{ma}-T_{ra}}{T_{oa}-T_{ra}}$ represents the outdoor air fraction, as explained in Eqn. 2. The term $\ln\left(\frac{x_{3,mb}}{\frac{T_{ma}-T_{ra}}{T_{oa}-T_{ra}}}\right) - x_{2,mb}$ is derived from Eqn. 1 to estimate the expected mixing box damper position in the economizer state to attain a T_{sa} without using the heating and cooling coils. If the mean absolute difference between the expected and measured mixing box damper command is greater than 20%, a state of operation fault alarm is generated.

Mode of operation

A VAV AHU system's routine operation is divided into six modes: occupied, unoccupied, set-up, set-back, warm-up, and cool-down modes (ASHRAE, 2018). Warm-up and cool-down periods are intended as transition from the unoccupied mode temperatures to the occupied mode temperature setpoints.

Set-up and set-back modes wake up a VAV AHU system in the unoccupied mode if the temperature of one or more zones gets colder than the unoccupied mode heating setpoint or warmer than the unoccupied mode cooling setpoint. While it is normal to see a VAV AHU occasionally operating in the set-up and set-back modes, on most days, AHU fans are expected to wake up once in the morning at the beginning of the warm-up/cool-down mode and turn off once in the evening at the end of the occupied mode. Therefore, the software tool generates a mode of operation fault if the fans experience more or less than two daily state changes on more than 50% of days.

SAT setpoint reset

As per ASHRAE Guideline 36 (2018), the SAT setpoint value should be dynamically reset to account for the heating and cooling demand from the zones. As the number of zones that requires space heating increases and those that require space cooling decrease, the SAT setpoint must increase. Similarly, as the demand for cooling increases, the SAT setpoint is expected to decrease. If the SAT setpoint is less than it should be, the economizer state will shift to colder outdoor temperatures. In the winter, this will increase the fraction of outdoor air in the supply air, increasing the space heating loads; and, in the shoulder seasons, this will reduce the fraction of outdoor air in the supply air, increasing the space cooling loads. If the SAT setpoint is greater than it should be, the fan electricity consumption in the summer and the risk of overheating in all seasons will increase. Correcting a faulty SAT reset logic can result in a 20-30% reduction in heating energy use (Hobson, 2020; Wei et al., 2005). The software tool generates an SAT setpoint reset fault alarm if it stays outside the acceptable SAT setpoint range defined by Gunay et al. (2020) for more than 20% of the operating hours.

<u>SAP setpoint reset</u>

SAP setpoint reset programs adjust the fan speed to account for the changes in the airflow demand from the VAV terminals. As more VAV terminal dampers open, indicating an increased demand for airflow, the SAP setpoint is expected to increase. As more dampers close, indicating a reduced demand for airflow, the SAP setpoint is expected to drop. Maintaining the SAP at setpoints higher than necessary will increase the fan electricity use, whereas maintaining it at setpoints less than needed will lead to zones not receiving adequate airflow. Addressing improper SAP setpoint reset programs generate 30-50% reductions in fan electricity use (Ma et al., 2015; Shea et al., 2019). The software tool generates an SAP setpoint reset fault alarm if more than five or less than two VAV terminal dampers are fully open on more than 20% of the operating time.

Implementation as a standalone application

The FDD algorithms presented so far were compiled as a Matlab function *ahuDoctor*. Subsequently, Matlab's App Designer tool was used to develop a GUI for the function (see Fig. 2). Lastly, Matlab's application compiler tool was used to implement *ahuDoctor* as a desktop application. The compiled application is standalone and does not require a Matlab installation. The executable file for installing *ahuDoctor* is provided as a supplemental file to this paper (DBOM, 2022). As shown in Fig. 2, *ahuDoctor* prompts to input trend data from a VAV AHU system, $s_{mb,dp,minsp}$, and seasonal availability of heating and cooling. It outputs fault alarms for the fault categories introduced earlier. It generates visualizations assisting the interpretation of the fault alarms. These visualizations are presented in the next section when demonstrating the FDD tool on a case study VAV AHU system. It outputs a KPI for the system health, which is calculated as one minus the fraction of the nine faults detected as follows:

$$KPI = 1 - \frac{f_{mb} + f_{hc} + f_{cc} + \frac{\sum_i^n \left(f_{vav,i} + f_{zn,i}\right)}{n} + f_{so} + f_{mo} + f_{sat} + f_{sap}}{9} \quad (7)$$

where f stands for the fault alarm status, and the subscripts mb, hc, cc, zn, so, and mo are the mixing box, heating coil, cooling coil, zone, state of operation, and mode of operation, respectively. The term n stands for the number of zones in the VAV AHU system. Recall that i is the zone index number. Lastly, the software tool generates a summary report containing the faults detected, relevant visualizations, and the KPI.

Demonstration of the FDD tool

The software tool is demonstrated with BAS data from a 69 zone VAV AHU system in an academic building in Ottawa, Canada. The data spans from August 8, 2017 to August 8, 2018. The trend data required by *ahuDoctor* were downloaded through the API of the BAS and formatted as per the input requirements discussed in the previous section. The data used in this demonstration are included as supplemental files (DBOM, 2022).

Fig. 3 presents the visualization generated to explain the mixing box damper fault alarm. A mixing box damper VAV AHU system fault alarm was generated because the fitted outdoor air fraction to mixing box damper command signal curve, defined in Eqn. 1, was partially outside the expected range of operation for parallel blade dampers (AMCA, 2009).

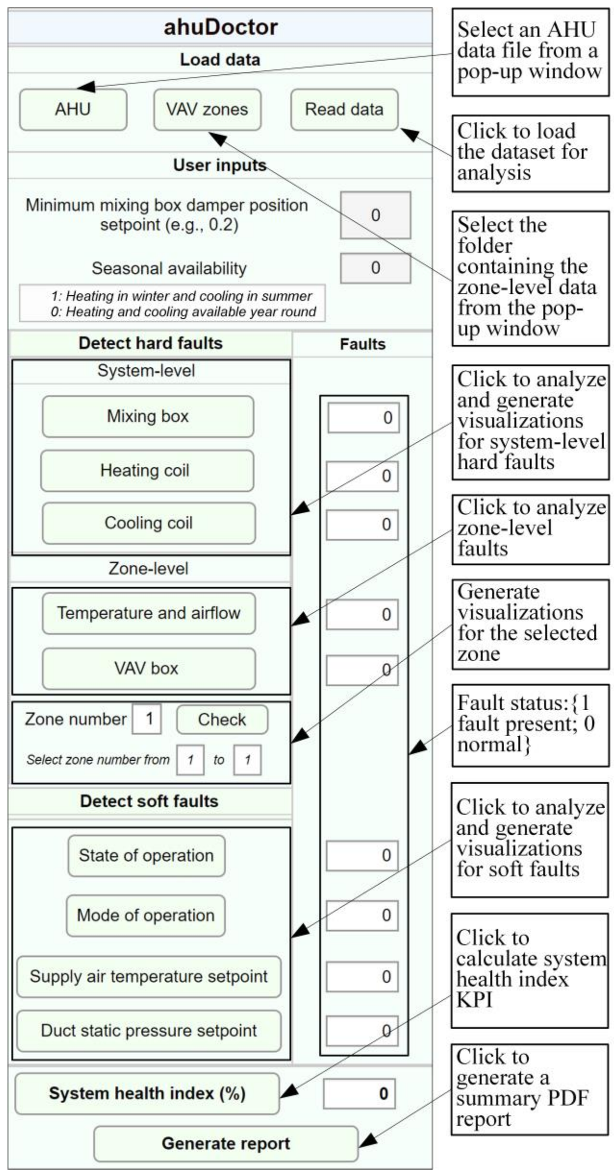

Figure 2:The GUI of the software tool.

Fig. 4 presents the visualizations generated to interpret heating and cooling coil valve faults. The software tool generated a fault alarm for the heating coil valve because the predicted temperature rise across the fully open heating coil, defined in Eqn. 4, was less than 5°C. The cooling coil valve was observed operating normally.

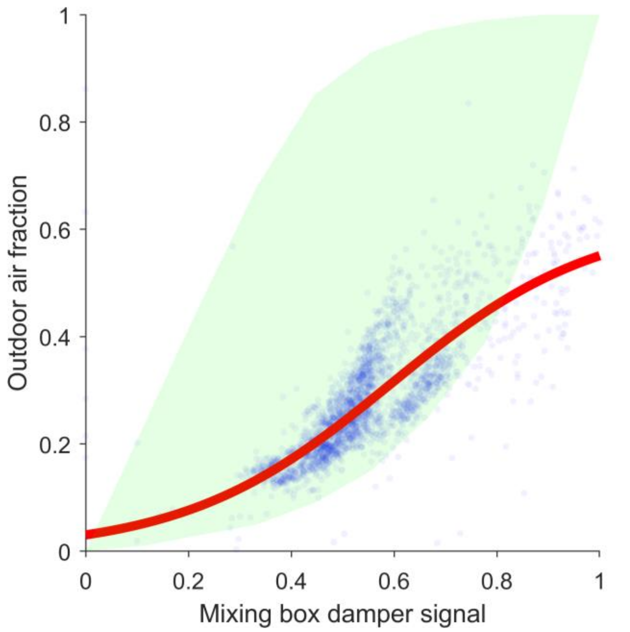

Figure 3: The mixing box damper signal to outdoor air fraction relationship. The red line represents the model defined in Eqn. 1. Green shaded region is the acceptable range as per AMCA (2009).

Fig. 5 presents mean airflow control error and the temperature for the winter and summer months separately. The tool detects that 26 of the 69 offices experienced temperature and airflow control anomalies. These zones either consistently could not control the airflow rate within 20% of the setpoint during the operating hours or maintained an average zone temperature less than 20°C or more than 25°C. Note that these zones had a default temperature setpoint of 22°C in the winter and 23.5°C in the summer. High temperature and airflow control errors are likely due to zone-level issues in the reheat coil or other perimeter heating devices and inappropriate discharge airflow setpoints.

Fig. 6 presents the damper position to discharge airflow relationship for two of the 69 VAV terminals as defined in Eqn. 5. Of them, Fig. 6(b) represents an example of a faulty VAV terminal unit. In total, three of the 69 zones were detected having a faulty VAV terminal unit. The faulty VAV terminal units did not experience an increase in their discharge airflow rate when their dampers opened, or the SAP increased. A VAV terminal unit fault may indicate an issue in the damper or the airflow sensor. Therefore, the appropriate action is to inspect them both if the tool generates this fault for a specific terminal.

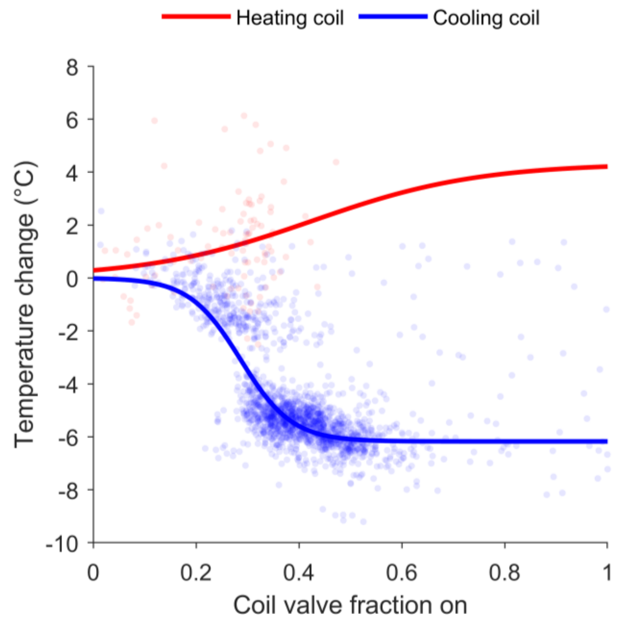

Figure 4: The temperature change across the heating and cooling coils. The solid lines represent the models defined in Eqn. 4.

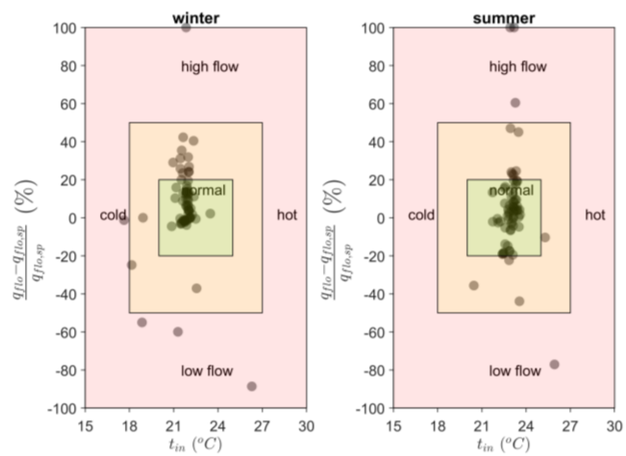

Figure 5: Normalized discharge airflow and temperature control error. Each scatter point represents a different VAV zone. Green, yellow, and red regions indicate normal, partially anomalous, and anomalous, respectively.

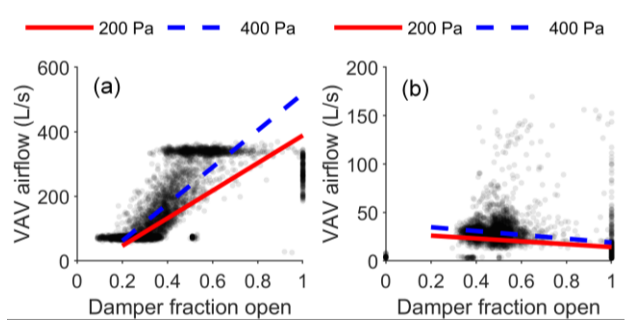

Figure 6: An example of (a) a normal and (b) a faulty relationship between VAV terminal damper opening fraction and discharge airflow rate. The line fits are defined in Eqn. 5.

Fig. 7 presents the expected and measured mixing box damper position with respect to the outdoor temperature. Recall that the expected mixing box damper position is determined as described in Eqn. 6, which employs the mixing box model (see Fig. 3 and Eqn. 1) together with ASHRAE Guideline 36 definitions for a VAV AHU system's states of operation (ASHRAE, 2018). The software tool did not generate a state of operation fault alarm because the mean absolute difference between the expected and measured mixing box damper positions was 14%, which was less than the built-in 20% alarm threshold defined in the tool.

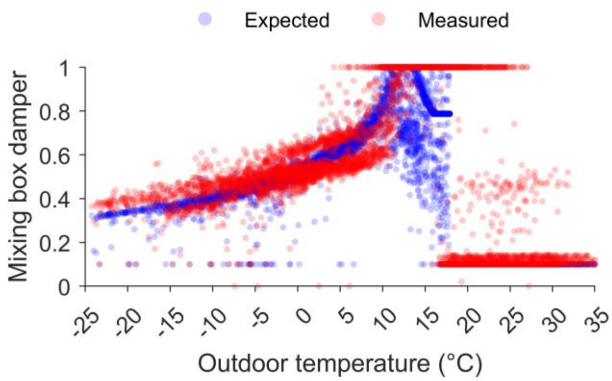

Figure 7: The expected and measured mixing box damper position with respect to the outdoor temperature. The expected damper position is determined using Eqn. 6.

Fig. 8 presents the distribution of fan state changes per day. On 60% of the days, the AHU fans experience two state changes (they turn on and off only once). On 32% of the days, the AHU fans experienced zero daily fan state changes and constantly operated the entire day. Because the VAV AHU system followed the weekly operating schedule by turning on and off only once on more than 50% of the days, the software tool did not generate a mode of operation fault alarm. The visualization generated by the software tool also indicates that fan switch on and off events were consistently happening at 7 am and 9 pm on most days, respectively.

Fig. 9 presents the measured and expected range of SAT as a function of the outdoor air temperature. Recall that the expected SAT range is extracted from Gunay et al. (2020). Notably, the outdoor air temperature-based SAT setpoint reset strategies previously reported in the literature also remain within this range (Park et al., 2020; Wei et al., 2005). The results indicate that the AHU did not employ an SAT setpoint reset sequence and operated outside the expected SAT range on 60% of the operating time. Higher than expected SAT values in the summer caused higher fan speeds to meet the cooling demand and contributed to the overheating in the summer (see Fig. 6). In contrast, lower than expected SAT values in the winter extended the economizer state into extremely cold outdoor temperatures – see the mixing box dampers open more than the minimum position even at temperatures less than -20°C in Fig. 7. This increased the use of perimeter heating to keep up with the cold supply air. Thus, the software tool generated an SAT setpoint reset alarm.

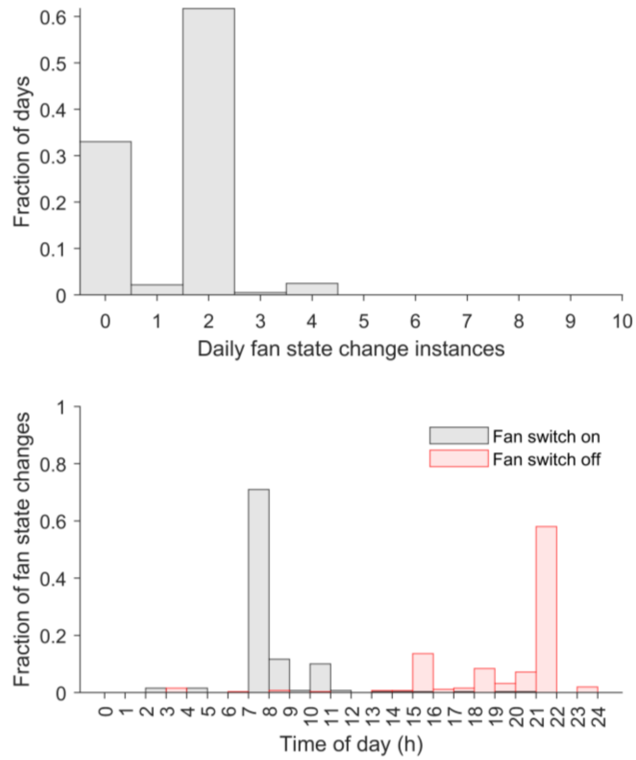

Figure 8: Histogram plots presenting the frequency of daily fan state changes and the temporal distribution of the fan switch on/off instances.

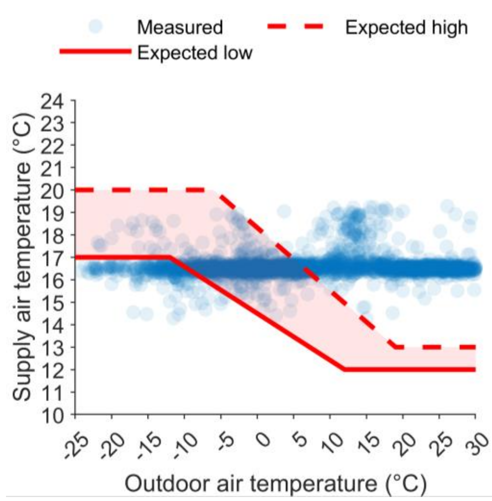

Figure 9: Measured and expected range of SAT as a function of the outdoor temperature. The expected range of SAT is taken from (Gunay et al., 2020).

Fig. 10 presents the distribution of the number of VAV terminal unit dampers fully open during the operating hours. Recall that a correct SAP setpoint reset program would continuously adjust the fan speeds while maintaining the number of fully open dampers at a reasonably low number, herein between two and five. All VAV terminal dampers will be partially closed when the SAP is unnecessarily high. When the SAP is less than needed, there will be many VAV terminals with fully open dampers. While the former case wastes fan electricity, the latter detrimentally affects the thermal comfort and indoor air quality. The results indicate that the case study VAV AHU system maintained the number of fully open VAV terminal dampers between two and five at about 85% of the time. Thus, the software tool did not generate an SAP setpoint reset logic fault alarm.

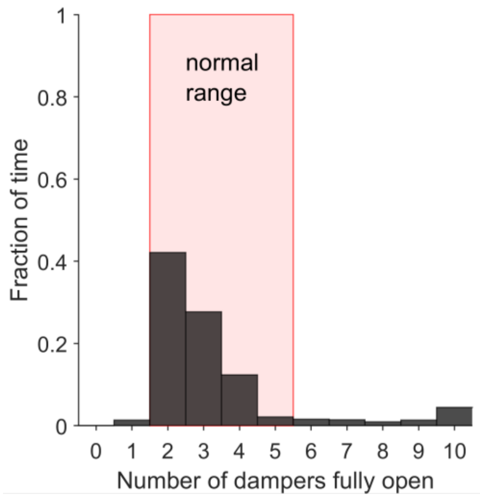

Figure 10: A histogram plot presenting the measured and expected range of the number of fully open dampers.

In summary, when employed on an actual multiple zone VAV AHU system, the *ahuDoctor* generated the following alarms: a mixing box damper fault, a heating coil valve fault, three terminal units with faulty dampers, 26 zones with airflow or temperature high control errors, and a supply air temperature setpoint reset logic fault. These represent five of the nine fault types covered by the software tool. Aside from generating the fault alarms and visualizations presented from Fig. 3 to 10, the *ahuDoctor* calculated the system health index KPI defined in Eqn. 7 as 62%. This KPI can be used to track the performance of a VAV AHU system over time and compare its performance to other systems in a building cluster. It can help facilities management teams prioritize preventive maintenance activities for underperforming VAV AHU systems.

Discussion

The software tool is presented as a standalone application whereby a user inputs historical data files on an ad-hoc basis to detect faults and generate visualizations and a KPI. Future iterations of *ahuDoctor* can be integrated into real-time data streams of a BAS, enabling batch periodic online data processing. With batch periodic online data processing, the tool can be implemented to a server with read access to a BAS. The server will periodically retrieve the most recent relevant archived BAS data, re-train the algorithms, and generate appropriate visualizations, fault alarms, and KPI.

The software tool was demonstrated with a year-long dataset. Given the practical importance of using the tool with a few weeks or months of data, an important line of inquiry for future work is identifying the minimum acceptable length of the dataset. For now, we recommend using a minimum of six months' worth of data to ensure coverage into both heating and cooling seasons.

The software tool employed inverse models for data assimilation. Trained models and ASHRAE Guideline 36 (2018) definitions were used to construct the expected operational behaviour. The tool generated a fault alarm when the difference between expected and measured operational behaviour exceeds a certain threshold. For example, a state of operation logic fault alarm was generated when the mean absolute difference between the expected and measured mixing box damper position was less than 20%. Future work should investigate the impact that alarm thresholds have on fault detection accuracy.

The current version of *ahuDoctor* is intended for multiple zone VAV AHU systems without any heat recovery or preheating devices. The mixing box model will need to be modified for systems with a heat recovery device. Further, the tool was developed with sensors and actuators that are essential for controlling AHU supply airflow and temperature, VAV discharge airflow, and zone temperature. Modern VAV AHU systems often feature more sensors for monitoring purposes, even though they are used for controls. These additional sensors can improve the detectability of faults. Future iterations of *ahuDoctor* should accommodate VAV AHU systems with different sensor configurations.

Conclusion

A software tool *ahuDoctor* was built upon state-of-the-art inverse model-based FDD algorithms for multiple zone VAV AHU systems. The tool inputs BAS trend data to develop inverse models representing the sensible heat and air mass transfer in AHU mixing boxes, heating and cooling coils, and VAV terminals. The inverse models are first used to detect hard faults. Subsequently, they are used to construct the expected operational behaviour based on ASHRAE Guideline 36 (2018) definitions. The mismatch between expected and measured operational patterns is treated as symptoms of soft faults. The *ahuDoctor* also generated visualizations and a system health index KPI.

The tool was demonstrated on a 69 zone VAV AHU system. The tool detected a mixing box damper fault, a heating coil valve fault, three terminal units with faulty dampers, 26 zones with airflow or temperature high control errors, and a supply air temperature setpoint reset logic fault.

Acknowledgement

This research is supported by a research contract with the National Research Council Canada.

References

AMCA (2009). 502-06 Damper application manual for heating, ventilating, and air conditioning. In. Arlington Heights: Air Movement and Control Association.

ASHRAE (2018). Guideline 36: High performance sequences of operation for HVAC systems. In. Atlanta: American Society of Heating, Refrigerating and Air-Conditioning Engineers.

Bruton, K., Coakley, D., Raftery, P., Cusack, D., Keane, M., & O'Sullivan, D. (2015). Comparative analysis of the AHU InFO fault detection and diagnostic expert tool for AHUs with APAR. *Energy Efficiency*, *8*, 299-322.

Claridge, D. E., Turner, W., Liu, M., Deng, S., Wei, G., Culp, C., Chen, H., & Cho, S. (2004). Is commissioning once enough? *Energy Engineering*, *101*, 7-19.

Darwazeh, D., Gunay, B., & Duquette, J. (2021). Development of Inverse Greybox Model-Based Virtual Meters for Air Handling Units. *IEEE Transactions on Automation Science and Engineering*, *18*, 323-336.

DBOM. (2022). ahuDoctor. https://github.com/Carleton-DBOM-Research-Group/ahuDoctor.

Granderson, J., Lin, G., Singla, R., Fernandes, S., & Touzani, S. (2018). Field evaluation of performance of HVAC optimization system in commercial buildings. *Energy and Buildings*, *173*, 577-586.

Gunay, B., Bursill, J., Huchuk, B., & Shillinglaw, S. (2022a). Inverse model-based detection of programming logic faults in multiple zone VAV AHU systems. *Building and Environment*.

Gunay, B., Newsham, G., Ashouri, A., & Wilton, I. (2020). Deriving sequences of operation for air handling units through building performance optimization. *Journal of Building Performance Simulation*, *13*, 501-515.

Gunay, B., Torabi, N., & Shillinglaw, S. (2022b). Classification of sequencing logic faults in multiple zone air handling units: a review and case study. *Science and Tech. for the Built Environment*.

Gunay, B., Shi, Z., Newsham, G., & Moromisato, R. (2020). Detection of zone sensor and actuator faults through inverse greybox modelling. *Bldg and Env.*, *171*, 106659.

Hobson, B. W. (2020). Development and implementation of occupancy-based predictive controls for modulation of air handling units' outdoor air dampers. MASc Thesis, Carleton University, Ottawa.

Kim, W., & Katipamula, S. (2018). A review of fault detection and diagnostics methods for building systems. *Science and Tech. for the Built Environment*, *24*, 3-21.

Ma, Y., Tukur, A., & Kissock, K. (2015). Energy-efficient static pressure reset in VAV systems. *ASHRAE Transactions*, *121*, 102.

Markus, A., Hobson, B., Gunay, B., & Bucking, S. (2021). A framework for a multi-sourced, data-driven building energy management toolkit. *Energy and Buildings*, 250, 111255.

Mills, E. (2011). Building commissioning: a golden opportunity for reducing energy costs and greenhouse gas emissions in the United States. *Energy Efficiency*, *4*, 145-173.

Mills, E., Bourassa, N., Piette, M. A., Friedman, H., Haasl, T., Powell, T., & Claridge, D. (2005). The cost-effectiveness of commissioning new and existing commercial buildings: Lessons from 224 buildings. Building Commissioning.

Mirnaghi, M. S., & Haghighat, F. (2020). Fault detection and diagnosis of large-scale HVAC systems in buildings using data-driven methods: A comprehensive review. *Energy and Buildings*, *229*, 110492.

Najafi, M., Auslander, D. M., Bartlett, P. L., Haves, P., & Sohn, M. D. (2012). Application of machine learning in the fault diagnostics of air handling units. *Applied Energy*, *96*, 347-358.

Padilla, M., Choinière, D., & Candanedo, J. A. (2015). A model-based strategy for self-correction of sensor faults in variable air volume air handling units. *Science and Tech. for the Built Environment*, *21*, 1018-1032.

Park, M.-K., Lee, J.-M., Kang, W.-H., Kim, C.-H., & Lee, K. H. (2020). Air-handling-unit discharge air temperature reset based on outdoor air temperature and cooling energy performance in an office building. *Energy Engineering*, *146*(3), 04020013.

Schein, J., Bushby, S. T., Castro, N. S., & House, J. (2006). A rule-based fault detection method for air handling units. *Energy and Buildings*, *38*(12), 1485-1492.

Shea, R. P., Kissock, K., & Selvacanabady, A. (2019). Reducing university air handling unit energy usage through controls-based energy efficiency measures. *Energy and Buildings*, *194*, 105-112.

Shi, Z., & O'Brien, W. (2019). Development and implementation of automated fault detection and diagnostics for building systems: A review. *Automation in Construction*, *104*, 215-229.

Torabi, N., Gunay, B., O'Brien, W., & Moromisato, R. (2021). Inverse model-based virtual sensors for detection of hard faults in air handling units. *Energy and Buildings*, *253*, 111493.

Wei, G., Claridge, D., Turner, W., & Liu, M. (2005). Choosing the right parameter for single-duct constant air volume system supply air temperature reset. *Architectural Engineering*, *11*, 76-80.